Three-body correlations in few-body nuclei

A. Arriaga

Centro de Fisica Nuclear da Universidade de Lisboa, Avenida Gama Pinto 2, 1699 Lisboa, Portugal

V.R. Pandharipande

Department of Physics, University of Illinois, Urbana, IL 61801, USA

R.B. Wiringa

Physics Division, Argonne National Laboratory, Argonne, IL 60439, USA

(February 9, 2008)

Abstract

A detailed comparison of Faddeev and variational wave functions for ^{3}H, calculated with realistic nuclear forces, has been made to study the form of three-body correlations in few-body nuclei. Three new three-body correlations for use in variational wave functions have been identified, which substantially reduce the difference with the Faddeev wave function. The difference between the variational upper bound and the Faddeev binding energy is reduced by half, to typically $< 2\%$. These three-body correlations also produce a significant lowering of the variational binding energy for ^{4}He and larger nuclei.

21.40.+d

I. INTRODUCTION

Quantum Monte Carlo methods, adopted for nuclei in the last decade, have proven to be very useful in obtaining exact solutions of the nuclear Schrödinger equation for the ground and low-energy excited states of up to six nucleons [1], and it is likely that many states of seven and eight nucleons will be exactly calculated with realistic nuclear forces in the near future. A variational approximation, $|\Psi_v\rangle$, to the lowest-energy state of the desired spin, parity, and isospin, (J^π, T), is first obtained by a variational Monte Carlo (VMC) calculation [2]. The exact eigenstate, $|\Psi_0\rangle$, belonging to the lowest-energy eigenvalue, E_0, for that (J^π, T) is then projected out using

$$|\Psi_0\rangle = \lim_{\tau\to\infty} exp[-(H - E_0)\tau]|\Psi_v\rangle \tag{1}$$

with the Green's function Monte Carlo (GFMC) method [3]. The computation yields a population of configurations $\mathbf{R}_i$, where $\mathbf{R} = (\mathbf{r}_1, \mathbf{r}_2, \cdots, \mathbf{r}_A)$ specifies the positions of all the nucleons and $i = 1, N_c$ labels the configurations, distributed with the probability

$$P(\mathbf{R}, \tau) \propto |\Psi_v^\dagger(\mathbf{R}) exp[-(H - E_0)\tau]\Psi_v(\mathbf{R})| \ . \tag{2}$$

Mixed estimates, defined as:

$$[O(\tau)]_M = \frac{\langle\Psi_v|O exp[-(H - E_0)\tau]|\Psi_v\rangle}{\langle\Psi_v|exp[-(H - E_0)\tau]|\Psi_v\rangle} \ , \tag{3}$$

are then calculated from this population. Obviously $[H(\tau)]_M$ converges to the eigenvalue E_0 in the limit $\tau \to \infty$, however, the variance of $[H(\tau)]_M$ depends primarily on that of the local variational energy:

$$E_v(\mathbf{R}) = \frac{\Psi_v^\dagger(\mathbf{R}) H \Psi_v(\mathbf{R})}{\Psi_v^\dagger(\mathbf{R})\Psi_v(\mathbf{R})} \ . \tag{4}$$

Expectation values of operators other than H are generally calculated only up to first order in the difference $(|\Psi_0\rangle - |\Psi_v\rangle)$ from

$$\langle O\rangle = 2 \lim_{\tau\to\infty}[O(\tau)]_M - \frac{\langle\Psi_v|O|\Psi_v\rangle}{\langle\Psi_v|\Psi_v\rangle} \ . \tag{5}$$

It is clear that accurate variational wave functions are needed for the success of this approach. The variance of $E_v(\mathbf{R})$ decreases and the terms neglected in eq.(5) become smaller as $|\Psi_v\rangle \rightarrow |\Psi_0\rangle$.

State-of-the-art variational wave functions [2] of few-body nuclei have the form:

$$|\Psi_v\rangle = [1 + \sum_{i<j} U_{ij}^{LS} + \sum_{i<j<k} U_{ijk}^{TNI}]|\Psi_p\rangle \tag{6}$$

with the pair wave function $|\Psi_p\rangle$ given by:

$$|\Psi_p\rangle = [S \prod_{i<j}(1 + U_{ij})]|\Psi_J\rangle \ . \tag{7}$$

The $S\prod_{i<j}$ represents a symmetrized product, and the Jastrow wave function, $|\Psi_J\rangle$, is given by:

$$|\Psi_J\rangle = \left[\prod_{i<j} f_c(r_{ij})\right] |\Phi\rangle \ . \tag{8}$$

Here $|\Phi\rangle$ is an antisymmetric product of single-particle wave functions with the desired (J^π, T), the $f_c(r_{ij})$ is a two-body central correlation, and the operator U_{ij} is defined as:

$$U_{ij} = \sum_{p=2,6} \left[\prod_{k\neq i,j} f_{ijk}^p(\mathbf{r}_{ik}, \mathbf{r}_{jk})\right] u_p(r_{ij}) O_{ij}^p \ , \tag{9}$$

$$O_{ij}^{p=1,6} = [1, \sigma_i \cdot \sigma_j, S_{ij}] \otimes [1, \tau_i \cdot \tau_j] \ . \tag{10}$$

The $f_c(r_{ij})$ and U_{ij} correlations are generated by the static parts of the two-nucleon interaction. The spin-orbit correlations are defined as:

$$U_{ij}^{LS} = [u_{\ell s}(r_{ij}) + u_{\ell s\tau}(r_{ij})\tau_i \cdot \tau_j](\mathbf{L}\cdot\mathbf{S})_{ij} \ , \tag{11}$$

and the eight radial functions $f_c(r_{ij})$, $u_{p=2,6}(r_{ij})$, $u_{\ell s}(r_{ij})$, and $u_{\ell s\tau}(r_{ij})$ are obtained from approximate two-body Euler-Lagrange equations with variational parameters [2]. The factor:

$$f_{ijk}^p = 1 - t_1 \left(\frac{r_{ij}}{R_{ijk}}\right)^{t_2} exp[-t_3 R_{ijk}] \ , \tag{12}$$

with

$$R_{ijk} = r_{ij} + r_{jk} + r_{ki} \ , \tag{13}$$

suppresses spin-isospin correlations between nucleons i and j when a third nucleon k comes close to either i or j, and t_{1-3} are variational parameters. Finally,

$$U_{ijk}^{TNI} = \epsilon V_{ijk}(\overline{r}_{ij}, \overline{r}_{jk}, \overline{r}_{ki}) \ , \tag{14}$$

with $\overline{r} = br$, represent correlations induced by the three-nucleon interaction $V_{ijk}(r_{ij}, r_{jk}, r_{ki})$. Its form is suggested by perturbation theory, and ϵ and b are variational parameters.

The exact ground-state energy of ^{3}H for the Argonne v_{14} two-nucleon [4] and Urbana model VIII three-nucleon [2] interactions, calculated using a Faddeev wave function [5] and Monte Carlo integration, is $-8.49(1)$, while the energy for ^{4}He, calculated by the GFMC [6] method, is $-28.3(2)$ MeV, where the numbers in parentheses denote the statistical error. VMC calculations [2] with the wave function of eq.(6) give instead the energies $-8.21(2)$ and $-27.23(6)$ MeV that are too high by $\sim 3.5\%$. This difference, reflecting the deficiencies in $|\Psi_v\rangle$, could be because the two-body functions f_c, u_p, $u_{\ell s}$, and $u_{\ell s\tau}$ are not optimally determined by the approximate equations used to construct them, or the true $|\Psi_0\rangle$ contains many-body correlations in addition to f_{ijk}^p and U_{ijk}^{TNI}. Note that a $|\Psi_v\rangle$ containing two- and three-body correlations can in principle reproduce the exact $|\Psi_0\rangle$ of ^{3}H.

We carried out extensive comparisons between the 34-channel Faddeev $|\Psi_F\rangle$ of the Los Alamos-Iowa group [5], one of the best available approximations to the exact $|\Psi_0\rangle$, and the $|\Psi_v\rangle$ for ^{3}H, to test the accuracy of the two-body functions in $|\Psi_v\rangle$ and study the three-body correlations in $|\Psi_F\rangle$, and therefore in $|\Psi_0\rangle$. These comparisons are discussed in Sec. II. Slight improvements in the two-body functions did not significantly reduce the difference $(|\Psi_F\rangle - |\Psi_v\rangle)$. However, a few three-body correlation operators can reduce this difference substantially. VMC calculations, for the binding energy of the three and four-body systems, with wave functions including the new correlations are presented in Sec. III. The error in these is approximately half of that in the best previous variational calculations [2].

II. COMPARISON OF THE FADDEEV AND VARIATIONAL WAVE FUNCTIONS AND THE NEW THREE-BODY CORRELATIONS

The new variational wave function we adopt is given by:

$$|\Psi_v\rangle = [1 + \sum_{i<j<k} U_{ijk} + \sum_{i<j} U_{ij}^{LS} + \sum_{i<j<k} U_{ijk}^{TNI}][\prod_{i<j<k} f_{ijk}^{c}]|\Psi_p\rangle \ , \tag{15}$$

and our purpose is to study the new three-body correlations, f_{ijk}^{c} and U_{ijk}, and also to improve the f_{ijk}^{p} correlations in $|\Psi_p\rangle$. We consider the triton wave function expressed in the spin-isospin basis

$$|\alpha\beta\rangle = |s_{12}sm\rangle|t_{12}\frac{1}{2}\frac{\overline{1}}{2}\rangle \ , \tag{16}$$

where s_{12} and t_{12} are respectively the total spin and isospin of the pair of particles (12), s is the total spin of the three nucleons, and m is its projection. Allowed values for s are $\frac{1}{2}$ (for $s_{12} = 0, 1$) and $\frac{3}{2}$ (for $s_{12} = 1$). The total isospin of the system is $\frac{1}{2}$, its projection is $\frac{\overline{1}}{2} \equiv -\frac{1}{2}$, and t_{12} can have the values 0 or 1. Consequently there are 16 components in the wave function, corresponding to the 8 spin states $|s_{12}sm\rangle$ labeled by $\alpha = 1, 8$ and the 2 isospin states $|t_{12}\frac{1}{2}\frac{\overline{1}}{2}\rangle$ labeled by $\beta = 1, 2$. These are defined as:

$$\begin{aligned}
|1\beta\rangle &= |0\frac{1}{2}\frac{1}{2}\rangle|\beta\rangle \ , \\
|2\beta\rangle &= |0\frac{1}{2}\frac{\overline{1}}{2}\rangle|\beta\rangle \ , \\
|3\beta\rangle &= |1\frac{1}{2}\frac{1}{2}\rangle|\beta\rangle \ , \\
|4\beta\rangle &= |1\frac{1}{2}\frac{\overline{1}}{2}\rangle|\beta\rangle \ , \\
|5\beta\rangle &= |1\frac{3}{2}\frac{3}{2}\rangle|\beta\rangle \ , \\
|6\beta\rangle &= |1\frac{3}{2}\frac{1}{2}\rangle|\beta\rangle \ , \\
|7\beta\rangle &= |1\frac{3}{2}\frac{\overline{1}}{2}\rangle|\beta\rangle \ , \\
|8\beta\rangle &= |1\frac{3}{2}\frac{\overline{3}}{2}\rangle|\beta\rangle \ ,
\end{aligned} \tag{17}$$

and

$$|\alpha 1\rangle = |\alpha\rangle|0\frac{1}{2}\frac{\overline{1}}{2}\rangle \ ,$$
$$|\alpha 2\rangle = |\alpha\rangle|1\frac{1}{2}\frac{\overline{1}}{2}\rangle \ . \tag{18}$$

The triton wave function at any configuration $\mathbf{R}$ can then be written as

$$\Psi(\mathbf{R}) = \sum_{\alpha,\beta} \psi_{\alpha\beta}(\mathbf{R})|\alpha\beta\rangle \tag{19}$$

The main components of the wave function are ψ_{31} and ψ_{12}, which are the only nonzero components in the Jastrow wave function. Other components are generated mostly by tensor and three-body correlations.

In order to determine the f^c_{ijk} and U_{ijk} we compared $|\Psi_v\rangle$ with $|\Psi_F\rangle$, and studied the deviations of the former relative to the latter. Using the decomposition of eq.(19) for both wave functions, we defined a number of "deviation" quantities. For each spatial configuration, $\mathbf{R}_k$, the deviation $\mathcal{E}_{\mathbf{R}_k}$ is given by

$$\mathcal{E}_{\mathbf{R}_k} = \sum_{\alpha\beta} |\psi_{v,\alpha\beta}(\mathbf{R}_k) - \psi_{F,\alpha\beta}(\mathbf{R}_k)|^2 \ . \tag{20}$$

Separately, we define a deviation $\mathcal{E}_{\alpha\beta}$ for each spin-isospin component

$$\mathcal{E}_{\alpha\beta} = \frac{1}{N}\sum_{k=1}^{N} |\psi_{v,\alpha\beta}(\mathbf{R}_k) - \psi_{F,\alpha\beta}(\mathbf{R}_k)|^2 \ , \tag{21}$$

where N is the total number of configurations considered. Finally, we define an average deviation $\mathcal{E}$

$$\mathcal{E} = \frac{1}{N}\sum_{k=1}^{N} \mathcal{E}_{\mathbf{R}_k} \ . \tag{22}$$

The exact $\Psi_0(\mathbf{R})$ satisfies $H\Psi_0(\mathbf{R}) = E_0\Psi_0(\mathbf{R})$ at all $\mathbf{R}$, however the $\Psi_F(\mathbf{R})$ does not satisfy this equation in all regions of configuration space, presumably due to the truncation in sums over partial waves and to interpolation between mesh points. In some regions $\Psi^\dagger_F(\mathbf{R})H\Psi_F(\mathbf{R})$ can be different from $E_0\Psi^\dagger_F(\mathbf{R})\Psi_F(\mathbf{R})$ by as much as 25%. For the study of the deviations listed above, a set of 1,000 configurations $\mathbf{R}_k$ for which $\Psi^\dagger_F(\mathbf{R})H\Psi_F(\mathbf{R})$ is within 5% of $E_0\Psi^\dagger_F(\mathbf{R})\Psi_F(\mathbf{R})$ was chosen from a larger set of random configurations distributed with the probability $\Psi^\dagger_F(\mathbf{R})\Psi_F(\mathbf{R})$.

We studied a wide variety of three-body correlations of the form $\xi(\mathbf{R})O_\xi$. For each O_ξ, values of $\xi(\mathbf{R}_k)$ were obtained by minimizing $\mathcal{E}_{\mathbf{R}_k}$. Simple functions of $\mathbf{R}$ were then chosen to approximate the extracted values of $\xi(\mathbf{R}_k)$. In principle, we can choose a set of sixteen operators O_ξ and define the complete three-body correlation as:

$$|\Psi_v\rangle = (1 + \sum_\xi \xi(\mathbf{R})O_\xi)|\Psi_p\rangle \tag{23}$$

instead of using eq. (15). The $\xi(\mathbf{R})$ can then be calculated by solving the matrix equation:

$$\left(\sum_\xi \xi(\mathbf{R})O_\xi\right)\psi_{p,\alpha\beta}(\mathbf{R}) = \psi_{F,\alpha\beta}(\mathbf{R}) - \psi_{p,\alpha\beta}(\mathbf{R}) \ , \tag{24}$$

obtained from $\Psi_v = \Psi_F$, at each value of $\mathbf{R}$. However, all our attempts led to unacceptable, rapidly fluctuating, functions $\xi(\mathbf{R})$ presumably dominated by the small differences between Ψ_F and the exact Ψ_0 and inappropriate choices of the sixteen operators O_ξ. In contrast, the $\xi(\mathbf{R})$ obtained by minimizing the deviation $\mathcal{E}_{\mathbf{R}_k}$ are smooth and useful for some of the operators O_ξ.

From the many operators O_ξ considered only a few produced a significant reduction of the deviations; we list below the successful ones. A spatial three-body correlation,

$$f^c_{ijk} = 1 + q^c_1(\mathbf{r}_{ij}\cdot\mathbf{r}_{ik})(\mathbf{r}_{ji}\cdot\mathbf{r}_{jk})(\mathbf{r}_{ki}\cdot\mathbf{r}_{kj})exp(-q^c_2 R_{ijk}) \ , \tag{25}$$

reduces the probability for particles i, j, and k to be in a line for $q^c_1 > 0$. The parameters of the new three-body correlations of type x are denoted by q^x_i; thus q^c_1 and q^c_2 are the parameters of f^c_{ijk}.

A spin-orbit three-body correlation

$$U^{\ell s}_{ijk} = \sum_{cyc} i\sigma_i\cdot(\mathbf{r}_{ij}\times\mathbf{r}_{ik})\left[\bar{v}_{ik}(\bar{f}'_{ij} - \bar{f}'_{jk}) - \bar{v}_{ij}(\bar{f}'_{ik} - \bar{f}'_{jk})\right] \ , \tag{26}$$

where

$$\bar{f}'(r) = q^{\ell s}_1 exp(-q^{\ell s}_2 r^2) \tag{27}$$

$$\bar{v}(r) = exp(-q^{\ell s}_3 r^2) \tag{28}$$

may be generated by the two-body spin-orbit interaction $\bar{v}(r_{ij})(\mathbf{L}\cdot\mathbf{S})_{ij}$ operating on the Jastrow correlations $\bar{f}(r_{ik})$ and $\bar{f}(r_{jk})$. It is expressed as a function of $\bar{v}$ and $\bar{f}$ to underline its motivation, however $\bar{v}$ differs significantly from the bare $\mathbf{L}\cdot\mathbf{S}$ potential and both $\bar{v}$ and $\bar{f}$ are determined by minimizing the $\mathcal{E}_{\mathbf{R}_k}$.

An isospin three-body correlation

$$U^{\tau}_{ijk} = \sum_{cyc}(\frac{1}{3}R_{ijk} - r_{ij})\left\{q^{\tau}_1 exp\left[-q^{\tau}_2(X_{ijk}-q^{\tau}_3)^2\right] - 2q^{\tau}_1 exp(-2q^{\tau}_2 X^2_{ijk})\right\}\tau_i\cdot\tau_j \ , \tag{29}$$

with

$$X_{ijk} = \left[1 + q^{\tau}_4(\hat{\mathbf{r}}_{ij}\cdot\hat{\mathbf{r}}_{ik})(\hat{\mathbf{r}}_{ji}\cdot\hat{\mathbf{r}}_{jk})(\hat{\mathbf{r}}_{ki}\cdot\hat{\mathbf{r}}_{kj})\right]R_{ijk} \ . \tag{30}$$

enhances the probability for $t_{ij}=0$ when nucleons i and j are far from k.

An example of a three-body correlation that we tried and found to be of marginal utility is given by:

$$U^{xt}_{ijk} = \sum_{cyc} i\sigma_i\cdot(\mathbf{r}_{ij}\times\mathbf{r}_{ik})\hat{\mathbf{r}}_{ij}\cdot\hat{\mathbf{r}}_{ik}\left[\bar{g}_{ij}\bar{g}_{ik}\right]i\tau_i\cdot(\tau_j\times\tau_k) \ , \tag{31}$$

where

$$\bar{g}(r) = q^{xt}_1 exp(-q^{xt}_2 r^2) \ . \tag{32}$$

Such a correlation may be generated by tensor interactions between pairs ij and ik. This correlation was omitted in our final energy calculations.

Finally, an improved parametrization of f^p_{ijk} was found, and eq.(12) is replaced by:

$$f^p_{ijk} = 1 - q^p_1(1-\hat{\mathbf{r}}_{ik}\cdot\hat{\mathbf{r}}_{jk})exp(-q^p_2 R_{ijk}) \ . \tag{33}$$

Initial values for the various parameters were obtained by minimizing $\mathcal{E}_{\mathbf{R}_k}$ for the test set of 1,000 Faddeev configurations. The final values of the parameters, which are somewhat different, are given in Table I; they were obtained by minimizing the binding energy of ^{3}H with the Argonne v_{14} and Urbana model VIII interactions for samples of 10,000 variational configurations.

To illustrate the procedure used to determine the form of the new correlation functions, we show in Fig. 1 the data points for the three-body central correlation $f^c_{ijk}(\mathbf{R})$ obtained by minimizing $\mathcal{E}_{\mathbf{R}_k}$ at each value of $\mathbf{R}$. These are for isosceles configurations $r_{13} = r_{23}$ with $R_{ijk} = 6$ fm, plotted against $cos\theta$, where θ is the angle formed by $\mathbf{r}_{13}$ and $\mathbf{r}_{23}$. The functional form of f^c_{ijk}, eq.(25), was chosen because it can fit these numerical values with appropriate parameters q^c_1 and q^c_2. The curve in Fig. 1 shows $f^c_{ijk}(\mathbf{R})$ with the slightly different values of q^c_1 and q^c_2 that minimize the energy; the data points and curve are quite similar.

The improvement achieved in the main components of Ψ_v can also be seen in Fig. 2 where we plot the difference $\psi_{F,31} - \psi_{v,31}$ for equilateral configurations as a function of R_{ijk}. The $\psi_{F,31} \times 10^{-2}$ is also shown in Fig. 2 for comparison. In this calculation the particles are placed in the xz-plane, where $\psi_{\alpha\beta}$ are real, and for equilateral configurations $\psi_{31} = -\psi_{12}$ holds exactly for antisymmetric Ψ. The difference $\psi_{F,31} - \psi_{v,31}$ is $\lesssim 1\%$ of $\psi_{F,31}$ for these configurations.

The average values of $|\psi_{F,\alpha\beta}|^2$, $\mathcal{E}_{\alpha\beta}$ [eq.(21)], $\Psi^\dagger_F\Psi_F$ and the total deviation $\mathcal{E}$ [eq.(22)] for the test set of 1,000 Faddeev configurations are listed in Table II for the new and old Ψ_v. They are normalized so that $\Psi^\dagger_F\Psi_F$ has unit average value for these configurations; note that this does not correspond to the standard normalization $\langle\Psi_F|\Psi_F\rangle = \langle\Psi_v|\Psi_v\rangle = 1$, however, it clearly exhibits the relative contributions and errors.

The main components, $\alpha\beta = 31$ and 12, have a rather small relative error, defined as $\mathcal{E}_{\alpha\beta}/\overline{|\Psi_{F,\alpha\beta}|^2}$, of $\sim 6 \times 10^{-5}$ in the new Ψ_v. Next in importance is the group of $s = \frac{3}{2}$ states ($\alpha = 5$ to 8) which have total orbital angular momentum $L_{tot} = 2$ and account for $\sim 12\%$ of $\overline{\Psi^\dagger_F\Psi_F}$. The largest of these have $\alpha\beta = 61$ and 72, and a relative error of $\sim 3 \times 10^{-4}$. The states $\alpha\beta = 71$ and 51 have smaller contributions, and a larger relative error of $\sim 10^{-2}$. The next group has $s = \frac{1}{2}$, $m = \frac{1}{2}$ where the pair of nucleons 1 and 2 is in an odd parity state. These states account for $\sim 0.1\%$ of $\overline{\Psi^\dagger_F\Psi_F}$ and have the largest relative error of $\sim 4 \times 10^{-2}$. The last group has $s = \frac{1}{2}$ and $m = -\frac{1}{2}$, for an $L_{tot} = 1$. It also accounts for $\sim 0.1\%$ of $\overline{\Psi^\dagger_F\Psi_F}$, and these components of the new Ψ_v have an error of $\sim 2 \times 10^{-2}$.

The $\mathcal{E}_{\alpha\beta}$ of the new Ψ_v are smaller than those of the old Ψ_v for all values of $\alpha\beta$ other

than 62. The total $\mathcal{E}$ of 0.00062 is reduced to 0.00047 by the new f^c_{ijk}. It is further reduced to 0.00035 by the inclusion of $U^{\ell s}_{ijk}$. The subsequent reduction to $\mathcal{E} = 0.00028$ is due to U^{τ}_{ijk}. The U^{xt}_{ijk} correlations and the changes in the f^p_{ijk} correlations have very small ($< 10^{-5}$) effect on the total $\mathcal{E}$.

III. BINDING ENERGY RESULTS FOR THE THREE- AND FOUR-BODY SYSTEMS; CONCLUSIONS

As mentioned in the previous section, the final values of the parameters of the new three-body correlations were determined by minimizing the energy. In Table III, we present the results for the binding energy of ^{3}H, for the Faddeev wave function and various variational wave functions moving from the old to the new. A set of 50,000 configurations sampled from $\langle \Psi_F | \Psi_F \rangle$ was used for these calculations. The first column contains the values of the binding energy and the second the difference $E_F - E_v$. We can clearly see that this difference is reduced approximately by a factor of two, when one goes from the old to the new Ψ_v, and that the f^c_{ijk} and $U^{\ell s}_{ijk}$ give almost 80% of the improvement.

The last column of Table III gives $\langle \Delta | \Delta \rangle$, where

$$|\Delta\rangle = |\Psi_F\rangle - |\Psi_v\rangle \ , \tag{34}$$

and $\langle \Psi_F | \Psi_F \rangle = \langle \Psi_v | \Psi_v \rangle = 1$. The $|\Delta\rangle$ gives the admixture of excited states in $|\Psi_v\rangle$. The mean energy of these excited states is given by:

$$\overline{E_x} \sim \frac{E_v - E_0}{\langle \Delta | \Delta \rangle} \sim 150 \ MeV \tag{35}$$

for both old and new Ψ_v. For this reason, the GFMC energy:

$$[E(\tau)] = \frac{\langle \Psi_v | H exp[-(H - E_0)\tau] | \Psi_v \rangle}{\langle \Psi_v | exp[-(H - E_0)\tau] | \Psi_v \rangle} \ , \tag{36}$$

of ^{3}H (and also ^{4}He) converges to the true E_0 by a rather small $\tau \sim 0.02$ MeV^{-1}. In contrast the Ψ_v of six-body nuclei seem to have admixtures of states with much smaller E_x, and their $E(\tau)$ does not converge so rapidly to E_0 as τ increases [1].

These new correlations, obtained by comparing the Ψ_F and Ψ_v for the Argonne v_{14} and Urbana VIII Hamiltonian, seem to have more general applicability. Results of variational calculations for ^{3}H and ^{4}He, with different interaction models, using either the old Ψ_v (Ref. [2]) or the new Ψ_v with the same three-body correlation parameters given in Table I are listed in Tables IV and V. (The difference between the old Argonne v_{14} and Urbana VIII value given in Table IV and the old f^p_{ijk} given in Table III is of marginal statistical significance; it can be attributed to slight changes to the the $|\Psi_p\rangle$ in the present work compared to Ref. [2], and the different random walks followed in the two calculations.) A significant improvement is seen in each case, with $\sim$ 30–50% of the energy difference with exact calculations, where available, recovered. In principle, the parameters of the new correlations should be optimized separately for each case, but this has not been done in the present work. The Faddeev energies shown in Table IV have been calculated from the Los Alamos-Iowa Ψ_F using Monte Carlo integration, and thus have a quoted statistical error. These energies are consistent with those published by the Los Alamos-Iowa group [5]. For ^{4}He, the current VMC results are fairly competitive with other recently developed methods, Faddeev-Yakubovsky (FY) [7] and correlated hyperspherical harmonics (CHH) [8], as shown in Table V. However, all these methods fall short of the exact GFMC calculations [6] in ^{4}He.

If the wave function $|\Psi\rangle$ were an exact eigenstate of H, then it should satisfy the eigenvalue equation:

$$H|\Psi\rangle = E|\Psi\rangle \tag{37}$$

and this equation should be satisfied for any space configuration, meaning that any local energy

$$E(\mathbf{R}) = \frac{\Psi^\dagger(\mathbf{R}) H \Psi(\mathbf{R})}{\Psi^\dagger(\mathbf{R})\Psi(\mathbf{R})} \tag{38}$$

should be equal to the eigenvalue E. For the three-body system we considered sets of different space configurations, each set being composed of configurations having the same R_{ijk} (the perimeter of the triangle formed by the three particles), and computed the average

of the energies returned by eq.(38). These average values, $\bar{E}$, are then a function of R_{ijk} and can be plotted against it. In Figs. 3, 4, and 5 we show the results respectively for the Faddeev wave function, and the old and new variational wave function. These calculations were done with the Argonne v_{14} two-body and Urbana model VIII three-body interactions.

From Fig. 3 we can clearly see that, even for the Faddeev wave function, there are regions, in particular for small and large perimeters, where the average values differ from the energy expectation value. Moreover, the variance is finite at all R_{ijk}, whereas it would be zero for an exact eigenfunction. The deviations of $\bar{E}(R_{ijk})$ and the variance of the Faddeev local energy are perhaps due to the errors introduced by numerical interpolation and the application of the permutation operators, required to go from the Faddeev amplitude to the full wave function, as explained in the previous section. The application of these permutation operators in the Los Alamos-Iowa Faddeev solution is implemented by means of partial wave series truncated at 34 channels. This problem led us to consider, in the procedure to search for the three-body correlations, only those regions in configuration space where the Faddeev wave function gives an $E(R)$ close to the exact energy. A comparison of the old and new variational wave function results (Fig. 4 to Fig. 5) shows that the new correlations clearly tend to push the average values in the right direction and to reduce the variance.

In variational calculations of six-body nuclei [1] the new three-body correlations continue to lower the variational upper bound. One simple generalization that can be made is to let the f^c_{ijk} correlation have different strengths depending on whether none, one, or two of the nucleons i, j, and k are in the p-shell. At present it appears best to let this correlation be zero if one or two are in the p-shell, although an alternate structure might be even better in these cases. It is also beneficial to reduce the overall strength of the $U^{\ell s}_{ijk}$ and U^{τ}_{ijk} correlations. With these steps, the new three-body correlations lower the energy by ~ 0.25 MeV in ^{6}Li, and also reduce the variance.

In conclusion we have reported significant progress in the construction of accurate variational wave functions for the nuclear few-body problem. We believe that the new three-body correlations will lead to clear improvement in GFMC wave functions for light nuclei, as well

as in variational wave functions of heavier systems.

ACKNOWLEDGMENTS

We wish to thank J.L. Friar, B.F. Gibson, and G.L. Payne for the use of their Faddeev wave functions. One of the authors (AA) would like to thank the kind hospitality of the Physics Department of the University of Illinois at Urbana-Champaign, where part of this work has been performed. The work of AA is supported by the University of Lisbon, Junta Nacional de Investigação Científica e Tecnológica under contract No. PBIC/C/CEN/1108/92, that of VRP by the National Science Foundation via grant PHY 94-21309, and that of RBW by the U.S. Department of Energy, Nuclear Physics Division, under contract No. W-31-109-ENG-38.

REFERENCES

[1] B. S. Pudliner, V. R. Pandharipande, J. Carlson, and R. B. Wiringa, Phys. Rev. Lett. **74**, 4396 (1995).

[2] R. B. Wiringa, Phys. Rev. C **43**, 1585 (1991).

[3] J. Carlson, Phys. Rev. C **38**, 1879 (1988).

[4] R. B. Wiringa, R. A. Smith, and T. L. Ainsworth, Phys. Rev. C **29**, 1207 (1984).

[5] C. R. Chen, G. L. Payne, J. L. Friar, and B. F. Gibson, Phys. Rev. C **31**, 2266 (1985); **33**, 1740 (1986); private communication.

[6] J. Carlson, Nucl. Phys. **A522**, 185c (1991).

[7] W. Glöckle and H. Kamada, Phys. Rev. Lett. **71**, 971 (1993); we have added 0.72 MeV to their published energy for the Coulomb interaction, the same amount obtained in the VMC calculation.

[8] M. Viviani, A. Kievsky, and S. Rosati, Few-Body Sys. **18**, 25 (1995).

FIGURES

FIG. 1. The three-body central correlation, $(f^c_{ijk} - 1)$ for isosceles configurations with $R_{ijk} = 6fm$, as a function of $cos\theta$, where θ is the angle formed by $\vec{r}_{13}$ and $\vec{r}_{23}$. The dots are the numerical values obtained by minimizing $\mathcal{E}_R$ and the full line shows the analytical function with parameters that minimize the energy.

FIG. 2. The difference $\psi_{F,31} - \psi_{v,31}$, for equilateral configurations, as a function of R_{ijk}. The dots and the diamonds correspond respectively to the old and new variational wave functions. The full line shows $\psi_{F,31}(\mathbf{R}_{ijk}) \times 10^{-2}$.

FIG. 3. Local energy E($\mathbf{R}$) of ^{3}H for 50,000 configurations of the Faddeev wave function, sampled with probability $|\Psi_F|^2$ and binned according to the perimeter variable R_{ijk}; the error bar denotes the variance in each bin. The horizontal line shows the average expectation value and the curve at the bottom shows the relative distribution of the samples as a function of R_{ijk}.

FIG. 4. Local energy E($\mathbf{R}$) of ^{3}H for 50,000 configurations of the old variational wave function; notation as in Fig. 3.

FIG. 5. Local energy E($\mathbf{R}$) of ^{3}H for 50,000 configurations of the new variational wave function; notation as in Fig. 3.

TABLES

TABLE I. Values of parameters in three-body correlation functions.

q_1^c	0.19	fm^{-6}
q_2^c	0.83	fm^{-1}
q_1^p	0.20	
q_2^p	0.06	fm^{-1}
$q_1^{\ell s}$	–0.12	fm^{-2}
$q_2^{\ell s}$	0.12	fm^{-2}
$q_3^{\ell s}$	0.85	fm^{-2}
q_1^τ	–0.014	fm^{-1}
q_2^τ	0.016	fm^{-2}
q_3^τ	1.2	fm
q_4^τ	0.25	

TABLE II. Average values of the wave functions and deviations.

$\alpha\beta$	s_{12}	t_{12}	s	m	$\overline{\lvert\Psi_{F,\alpha\beta}\rvert^2}$	$\mathcal{E}_{\alpha\beta,new}$	$\mathcal{E}_{\alpha\beta,old}$
31	1	0	$\frac{1}{2}$	$\frac{1}{2}$	4.4×10^{-1}	2.7×10^{-5}	1.2×10^{-4}
12	0	1	$\frac{1}{2}$	$\frac{1}{2}$	4.4×10^{-1}	2.7×10^{-5}	1.1×10^{-4}
61	1	0	$\frac{3}{2}$	$\frac{1}{2}$	4.1×10^{-2}	1.6×10^{-5}	1.8×10^{-5}
72	1	1	$\frac{3}{2}$	$-\frac{1}{2}$	3.0×10^{-2}	7.2×10^{-6}	2.2×10^{-5}
81	1	0	$\frac{3}{2}$	$-\frac{3}{2}$	1.3×10^{-2}	3.8×10^{-5}	4.6×10^{-5}
52	1	1	$\frac{3}{2}$	$\frac{3}{2}$	1.2×10^{-2}	1.8×10^{-5}	5.1×10^{-5}
62	1	1	$\frac{3}{2}$	$\frac{1}{2}$	1.2×10^{-2}	4.7×10^{-5}	4.2×10^{-5}
82	1	1	$\frac{3}{2}$	$-\frac{3}{2}$	4.3×10^{-3}	1.4×10^{-5}	2.4×10^{-5}
71	1	0	$\frac{3}{2}$	$-\frac{1}{2}$	2.2×10^{-3}	1.5×10^{-5}	2.2×10^{-5}
51	1	0	$\frac{3}{2}$	$\frac{3}{2}$	2.0×10^{-3}	1.7×10^{-5}	5.0×10^{-5}
11	0	0	$\frac{1}{2}$	$\frac{1}{2}$	4.6×10^{-4}	1.7×10^{-5}	2.9×10^{-5}
32	1	1	$\frac{1}{2}$	$\frac{1}{2}$	4.6×10^{-4}	1.7×10^{-5}	2.9×10^{-5}
42	1	1	$\frac{1}{2}$	$-\frac{1}{2}$	3.9×10^{-4}	5.6×10^{-6}	8.7×10^{-6}
21	0	0	$\frac{1}{2}$	$-\frac{1}{2}$	3.8×10^{-4}	5.4×10^{-6}	8.7×10^{-6}
41	1	0	$\frac{1}{2}$	$-\frac{1}{2}$	2.5×10^{-4}	7.4×10^{-6}	2.5×10^{-5}
22	0	1	$\frac{1}{2}$	$-\frac{1}{2}$	2.1×10^{-4}	9.2×10^{-6}	2.2×10^{-5}
sum					1.0	2.8×10^{-4}	6.2×10^{-4}

TABLE III. Comparison between binding energy values calculated with $|\Psi_F\rangle$ and the various $|\Psi_v\rangle$ described in the text.

Wave function	E	$E_v - E_F$	$\langle\Delta\|\Delta\rangle$
Faddeev	-8.479 (12)		
new $f^p_{ijk} + f^c_{ijk} + U^{\ell s}_{ijk} + U^{\tau}_{ijk}$	-8.354 (16)	.125 (19)	.00079
new $f^p_{ijk} + f^c_{ijk} + U^{\ell s}_{ijk}$	-8.346 (16)	.133 (19)	.00099
new $f^p_{ijk} + f^c_{ijk}$	-8.305 (15)	.175 (19)	.00111
new f^p_{ijk}	-8.260 (20)	.219 (23)	.00139
old f^p_{ijk}	-8.253 (19)	.227 (22)	.00146

TABLE IV. Binding energy in MeV for ^{3}H with old and new correlations.

Hamiltonian	Reid v_8	Argonne v_{14}	Argonne v_{14} + Tucson	Argonne v_{14} + Urbana VII	Argonne v_{14} + Urbana VIII
old[a]	7.31(2)	7.45(1)	8.80(3)	8.79(1)	8.21(2)
new	7.44(3)	7.53(2)	9.05(2)	8.95(1)	8.35(1)
Faddeev	7.59(2)	7.70(1)	9.33(2)	9.05(1)	8.49(1)

[a]Ref. [2]

TABLE V. Binding energy in MeV for ^{4}He with old and new correlations.

Hamiltonian	Reid v_8	Argonne v_{14}	Argonne v_{14} + Tucson	Argonne v_{14} + Urbana VII	Argonne v_{14} + Urbana VIII
old[a]	23.62(6)	23.54(4)	30.64(9)	30.51(4)	27.23(6)
new	24.01(8)	23.80(6)	31.69(9)	30.79(5)	27.63(5)
FY[b]		23.90			
CHH[c]		23.93			27.48
GFMC[d]	24.55(13)	24.2(2)			28.3(2)

[a]Ref. [2]

[b]Ref. [7]

[c]Ref. [8]

[d]Ref. [6]

Fig. 1 (Arriaga, Pandharipande, & Wiringa)

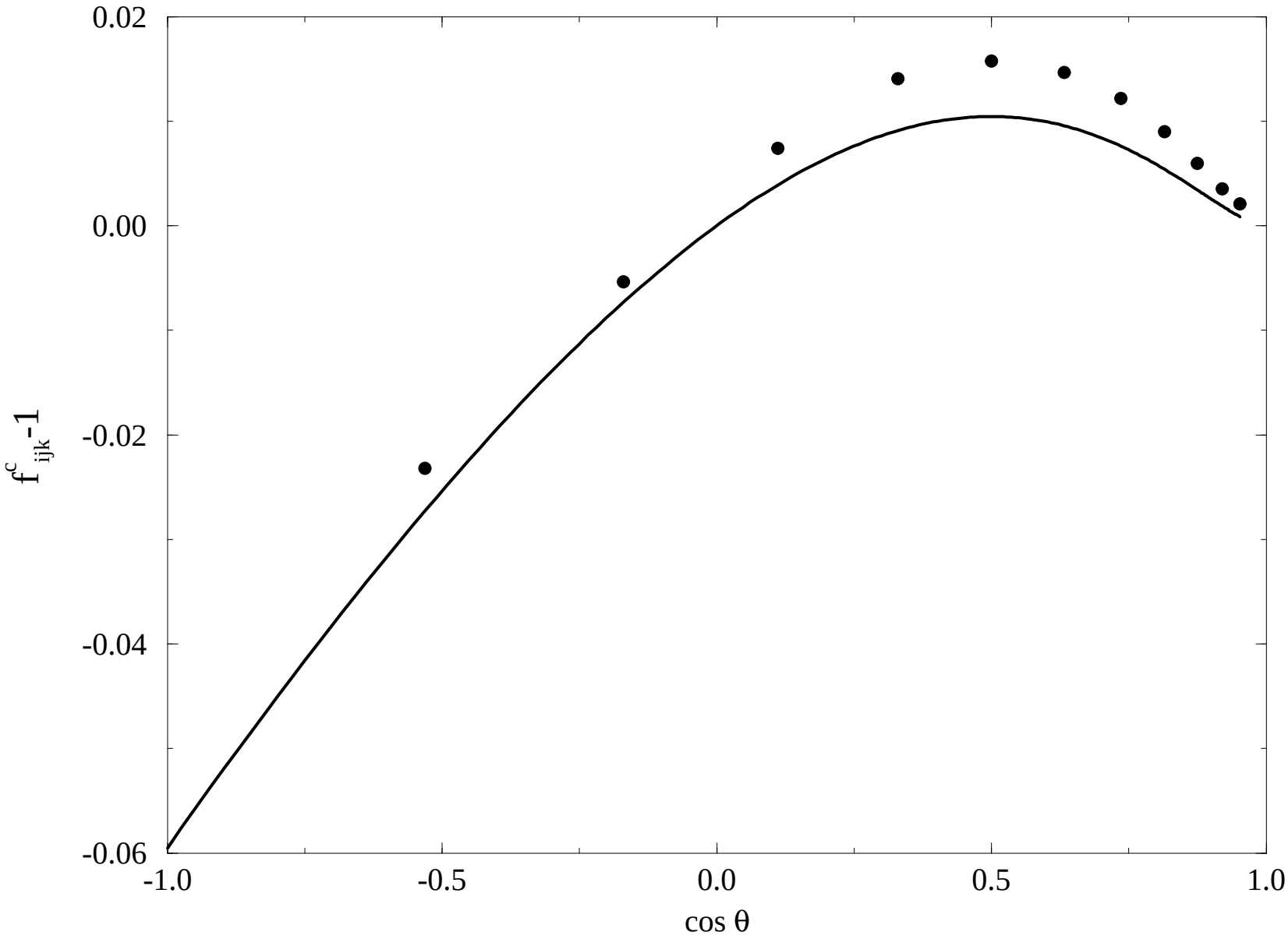

Fig. 2 (Arriaga, Pandharipande, & Wiringa)

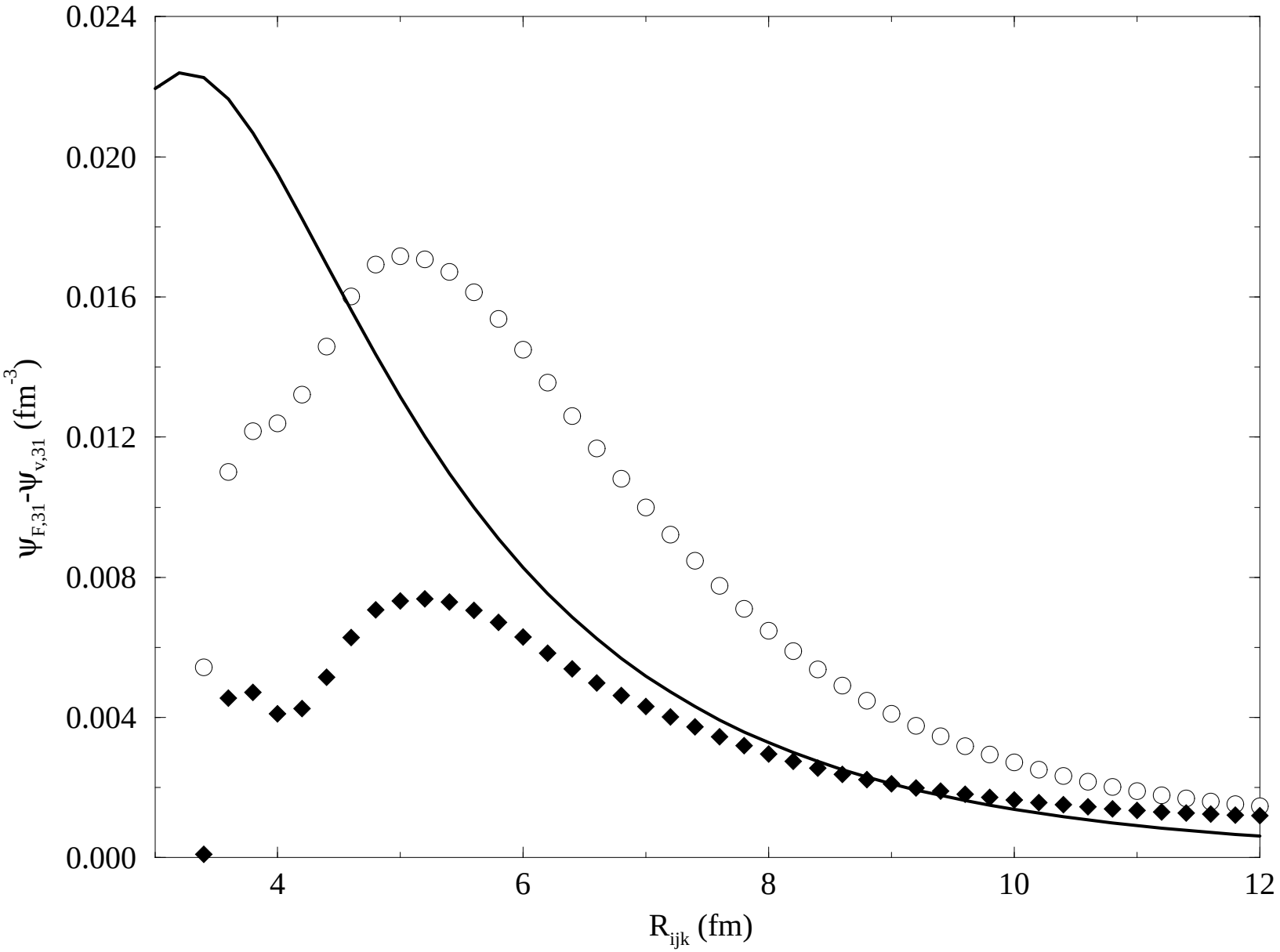

Fig. 3 (Arriaga, Pandharipande, & Wiringa)

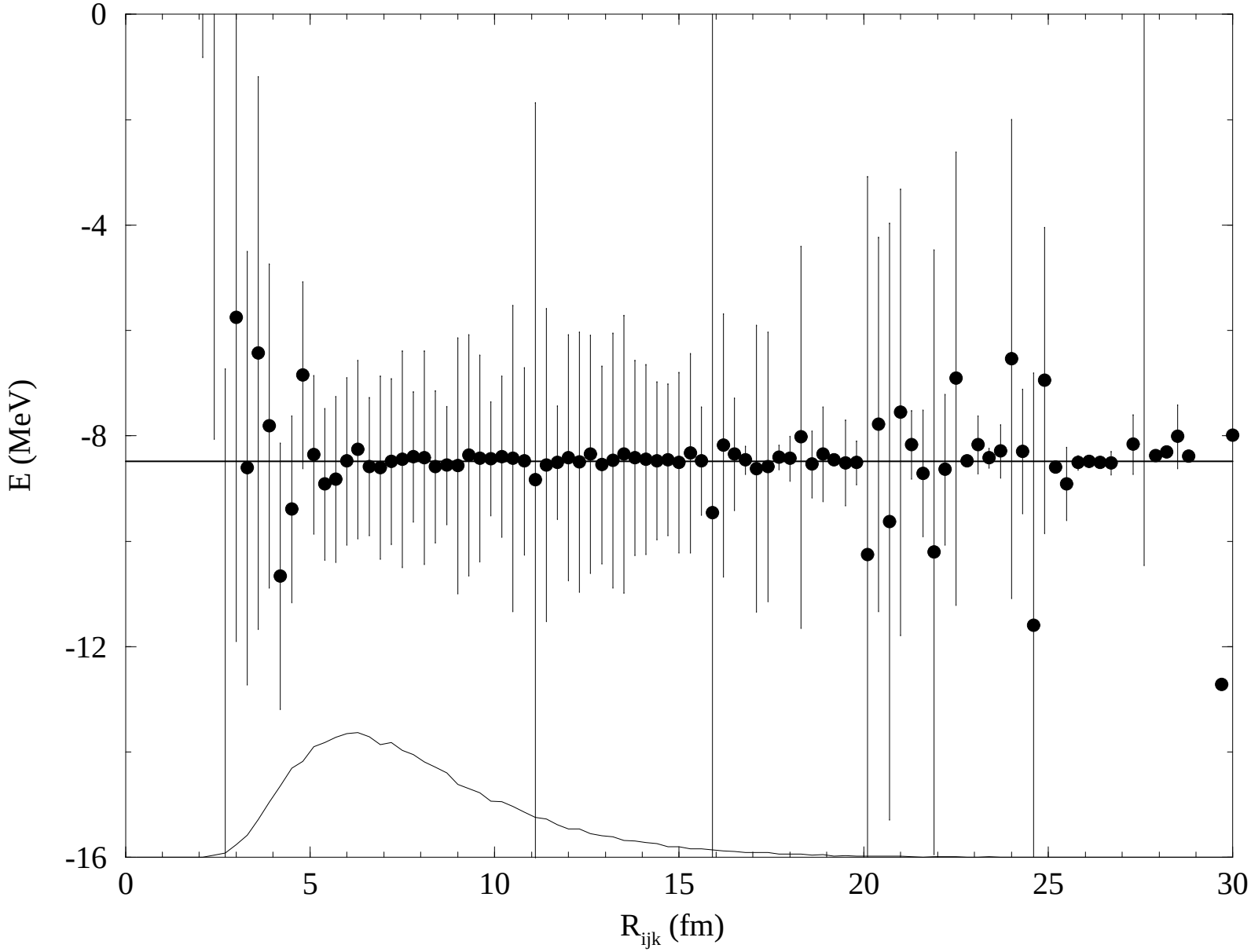

Fig. 4 (Arriaga, Pandharipande, & Wiringa)

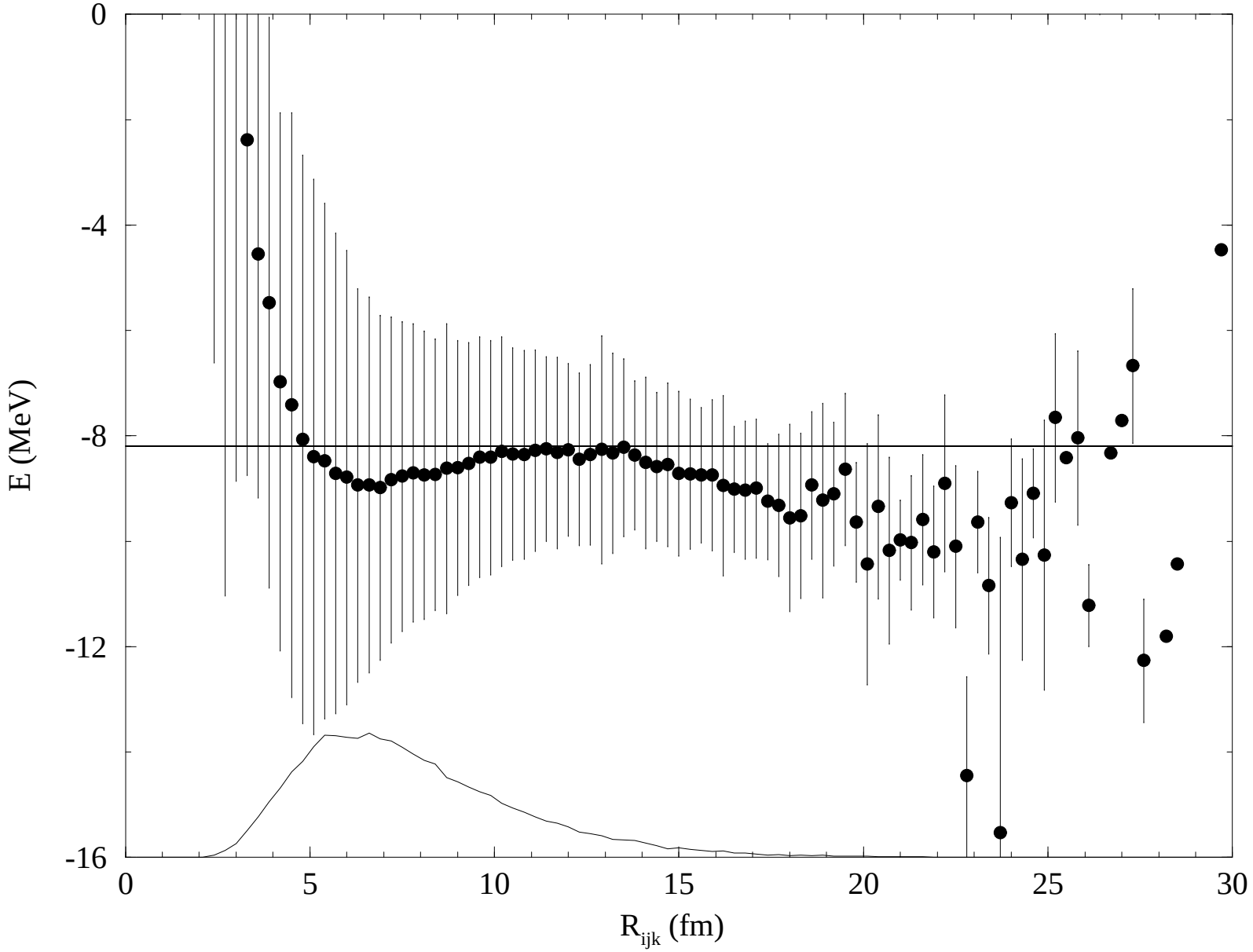

Fig. 5 (Arriaga, Pandharipande, & Wiringa)